Supporting Information:

Energetic landscape and terminal emitters of phycobilisome cores from quantum chemical modeling

Lorenzo Cupellini,[a,*] Michal Gwizdala[b,c,d], Tjaart P.J. Krüger[b,c]

[a] *Dipartimento di Chimica e Chimica Industriale, Università di Pisa, Via G. Moruzzi 13, 56124 Pisa, Italy*

[b] *Department of Physics, University of Pretoria, Lynnwood Road, Pretoria, 0002, South Africa*

[c] *Forestry and Agricultural Biotechnology Institute (FABI), University of Pretoria, Lynnwood Road, Pretoria, 0002, South Africa*

[e] *National Institute of Theoretical and Computational Sciences (NITheCS) South Africa*

S1 Validation of the computational strategy

To validate the strategy employed in this work, we calculated the exciton Hamiltonian for the (ApcD/ApcB)$_3$ trimer of **Scy. 6803**. The structure of this trimer was resolved at 1.75 Å resolution by Peng *et al.* (PDB: 4PO5)[1]. The same refinement and QM/MM optimization strategy adopted for the PB core trimers were used for this trimer.

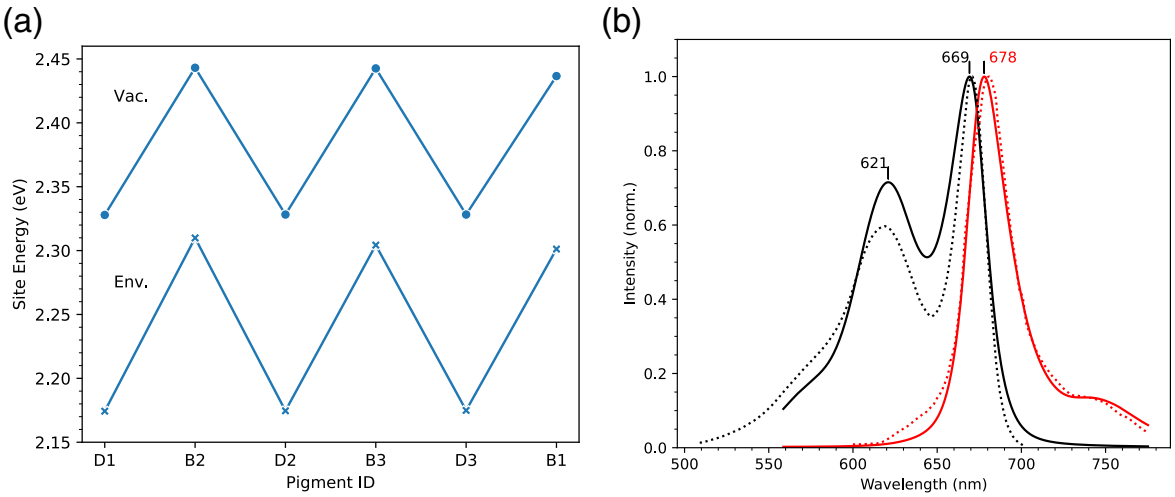

Fig. S1 Results on the ApcB/ApcD trimer of **Scy. 6803** (PDB: 4PO5). (a) Site energies of the six pigments (ApcD/ApcB) *in vacuo* (top) and in the protein environment (bottom). (b) Simulated absorption (black) and emission (red) spectra (solid lines). Experimental spectra from Ref. 1 are shown as dotted lines. The frequency axis was shifted by -2100 cm^{-1}. A static disorder of 30 cm^{-1} and 300 cm^{-1} was used for ApcD and ApcB, respectively, to match the shape of the experimental spectra.

The calculated site energies (Fig. S1a) show a clear pattern, which is expected given the symmetry of the complex. The ApcD pigments have a significantly red-shifted excitation energy (-0.13 eV, i.e., -1050 cm^{-1}) with respect to ApcB. Notably, the site energies calculated *in vacuo* and in the environment only differ by a systematic shift, meaning that the energy ladder is entirely determined by the internal geometry of the pigments. The ApcB-ApcD site energy gap is reflected in the simulated absorption spectrum (Fig. S1b), which shows two well-separated maxima whose split corresponds roughly to the site-energy difference between the two pigments.

To compare this spectrum with experiments, we applied a rigid shift to the frequencies, which accounts for the intrinsic and systematic error of our computational method. We determined a shift of -2100 cm^{-1} to reproduce the position of the lowest absorption band. Notably, the positions of all bands fall within 1 nm of the measured maxima[1]. This allowed us to determine the soundness of the computational strategy as well as the magnitude of the systematic error on the site energies (i.e., -2100 cm^{-1}). The site energy difference between ApcD and ApcB pigments is well captured (within 50 cm^{-1}) by our calculations.

S2 Structural determinants of the excitation energy

In order to understand how the excitation energy depends on geometrical parameters, we trained a simple linear model to fit the *in vacuo* excitation energy using more than one geometrical parameter. Specifically, we used the following expression:

$$E_{\mathrm{exc},i}^{(\mathrm{vac})} = E_0 + \Delta E_{\mathrm{ApcE}}\delta_{i,\mathrm{ApcE}} + b_1\cos(\phi_i^{CD}) + b_2\cos(\phi_i^{AB}) + b_3\alpha_i^{BC}, \tag{S1}$$

where i runs over all PCB chromophores computed in this work (from both structures), ϕ^{CD} is the value of the N_C=C_{14}-C_{15}=C_{16} dihedral angle, ϕ^{AB} is the value of the C_4=C_5-C_6=N_B dihedral angle, and α^{BC} is the value of the C_9=C_{10}-C_{11} angle. $\delta_{i,\mathrm{ApcE}} = 1$ for ApcE pigments and 0 otherwise, allowing a separate intercept for ApcE pigments. This is needed because only two ApcE pigments are present in the data set, which could skew the results. Alternatively, we performed the fit excluding ApcE pigments altogether. The fitting results with and without the

ApcE data are shown in Table S1.

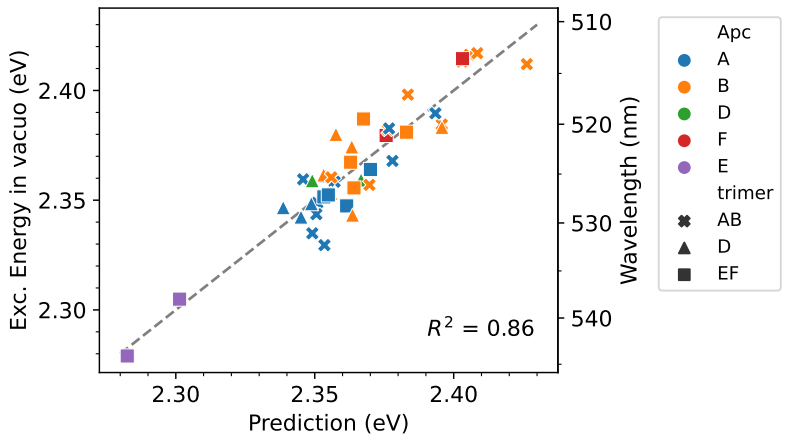

Fig. S2 Correlation between the *in vacuo* excitation energies of PCBs and a ordinary least squares prediction based on (i) the dihedral angles N_C=C_{14}-C_{15}=C_{16} and C_4=C_5-C_6=N_B and (ii) the angle C_9=C_{10}-C_{11}. A separate intercept was allowed for ApcE pigments. See text for details. The dashed line shows the $y = x$ diagonal and serves as a guide to the eye.

The results (Fig. S2) show a better linear correlation than using the dihedral ϕ^{CD} alone as in Figure **??** of the main text, although the obtained coefficient b_1 is similar to the coefficient of $\cos(\phi_i^{CD})$. The obtained coefficients do not change significantly when we exclude the ApcE pigments from the fit (Table S1). We also note that the coefficient of $\cos(\phi^{AB})$ is much smaller than that associated to $\cos(\phi^{CD})$. Given that the two dihedral angles have a similar variability, this means that the contribution of ϕ^{AB} to the excitation energy is marginal.

Table S1 Fitted coefficients for the model in eq. S1 with their relative standard error. The model without ApcE was fitted excluding ApcE pigments. All values are in eV; it is assumed that the angle α^{BC} is measured in degrees, whereas for the dihedral angles the cosine is calculated.

Geometrical parameter			**Including ApcE**		**Without ApcE**	
Parameter	Range	Coeff. name	Coeff. (eV)	Std. Error (eV)	Coeff. (eV)	Std. Error (eV)
Intercept	—	E_0	1.821	0.234	1.857	0.249
ApcE	—	ΔE_{ApcE}	−0.234	0.085	—	—
ϕ^{CD}	150–210°	b_1	0.575	0.054	0.572	0.055
ϕ^{AB}	140–180°	b_2	0.090	0.045	0.086	0.047
α^{BC}	131–136°	b_3	0.009	0.002	0.009	0.002

S3 Additional Figures

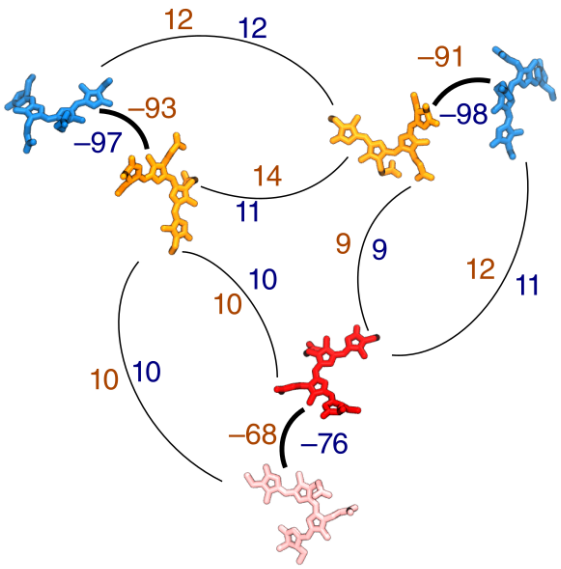

Fig. S3 Excitonic couplings within the **EF-trimer**. All values are in cm^{-1}, and couplings less than 5 cm^{-1} are not shown. Orange numbers refer to **Sco. 7002** while blue numbers refer to **Scy. 6803**. The orientation and colors of the PCB pigments are the same as in Figure **??**d.

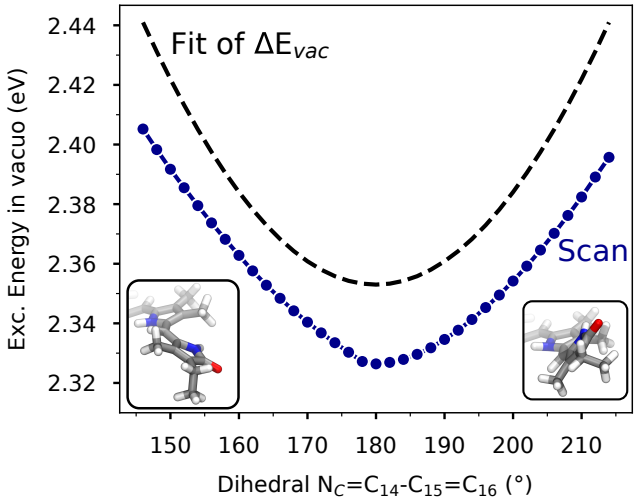

Fig. S4 Dependence of the excitation energy of a PCB model on the N_C=C_{14}-C_{15}=C_{16} torsion calculated on a relaxed geometry scan of PCB *in vacuo* (blue dots and line), compared with the fit of Figure **??**a, namely $f(x) = A + B(1 + \cos(\phi))$, with parameters $A = 2.348$ eV and $B = 0.571$ eV. The insets show the D-ring orientation in the first and last structure of the scan. Note that the PCB geometries in this scan differ from the ones in the protein because they have been relaxed without the protein environment.

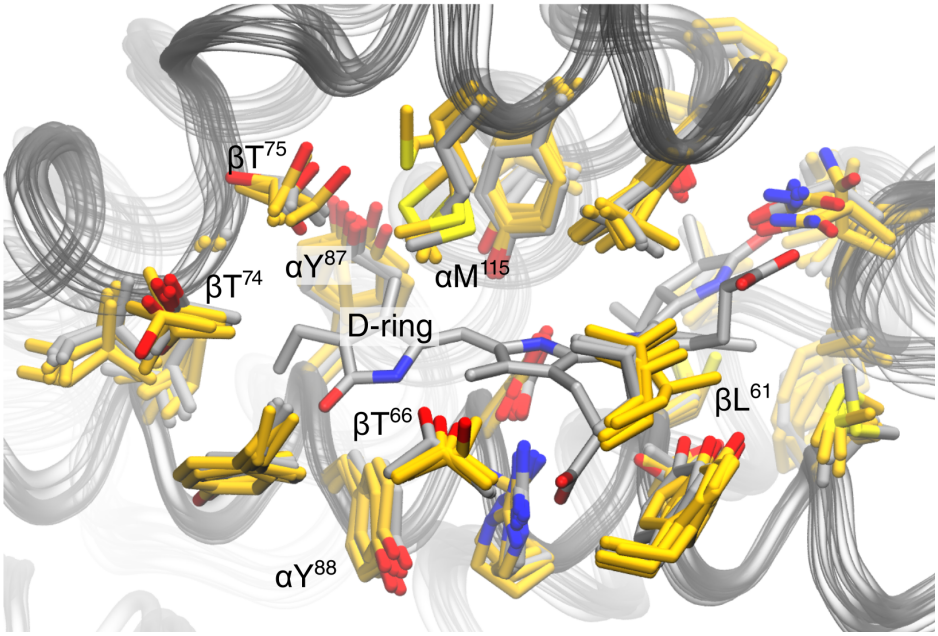

Fig. S5 Variability in the ApcA PCB-binding pocket in the **Scy. 6803** structure. Only one PCB is shown ($ApcA_1$ from the **AB-trimer**) for clarity and to show a case where the D-ring is significantly distorted. Gold-colored residues depict the pockets that give rise to blue-shifted ApcA (transition energy >2.20 eV). The labels refer to the ApcA (α) residues or to the ApcB (β) residues of the closest ApcB protomer. Refined geometries are shown here, but the picture is similar for the original PDB structure.

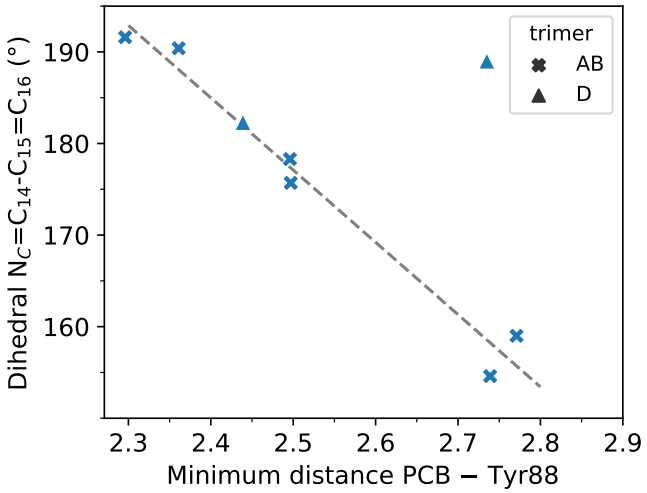

Fig. S6 Relationship between the D-ring dihedral ϕ^{CD} and the minimum distance between the bilin atoms and the atoms of Tyr88. The analysis has been performed for the same ApcA PCB-binding pockets in **Scy. 6803** shown in Figure S5. The dashed line shows a linear fit that excludes the outlier in the top-right corner.

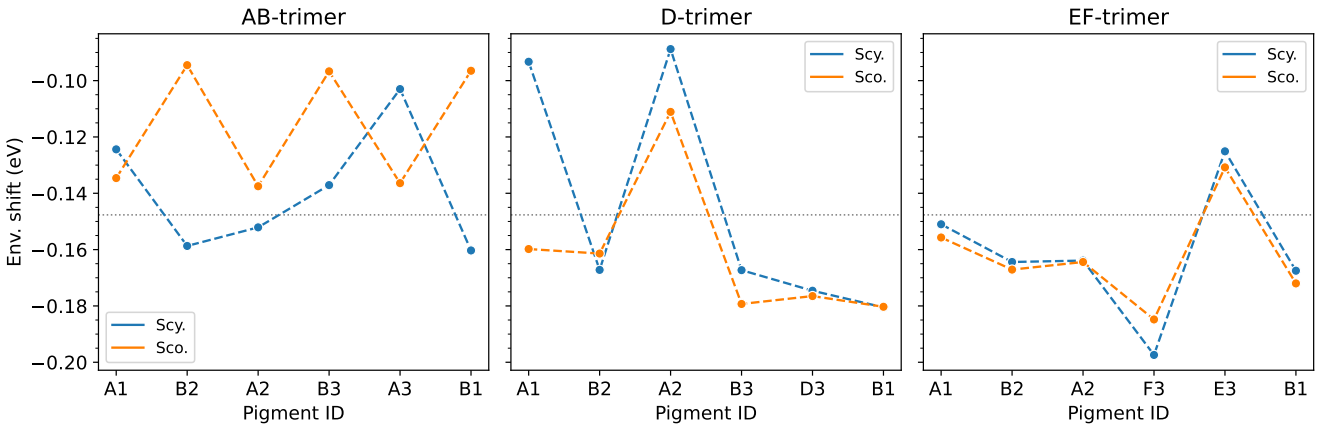

Fig. S7 Environment electrostatic shifts for the PB core trimers. The shifts are computed by subtracting the site energy calculated in environment and those calculated *in vacuo*. Orange lines refer to **Sco. 7002** while blue lines refer to **Scy. 6803**. The horizontal grey dotted line shows the average of all shifts and serves as a guide to the eye. Each Apc is labeled according to Figure ??b-d.

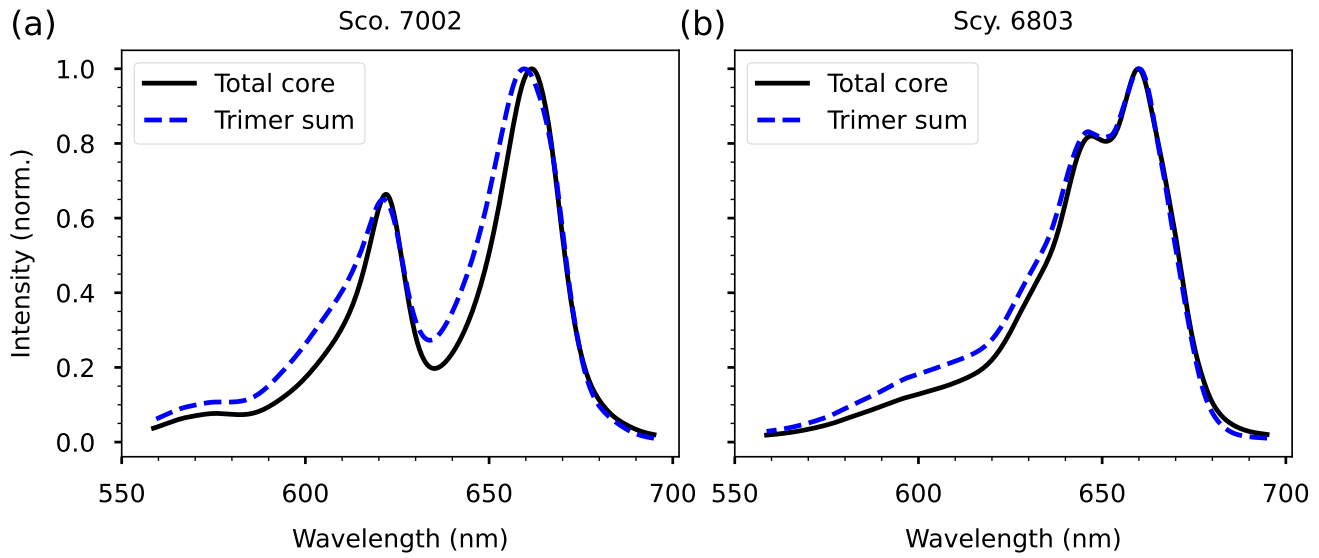

Fig. S8 Comparison of the 77 K absorption spectrum of the core calculated by including all excitonic interactions ("Total core") and the weighted sum of the constituting trimers ("Trimer sum") for the core of (a) **Sco. 7002** and (b) **Scy. 6803**.

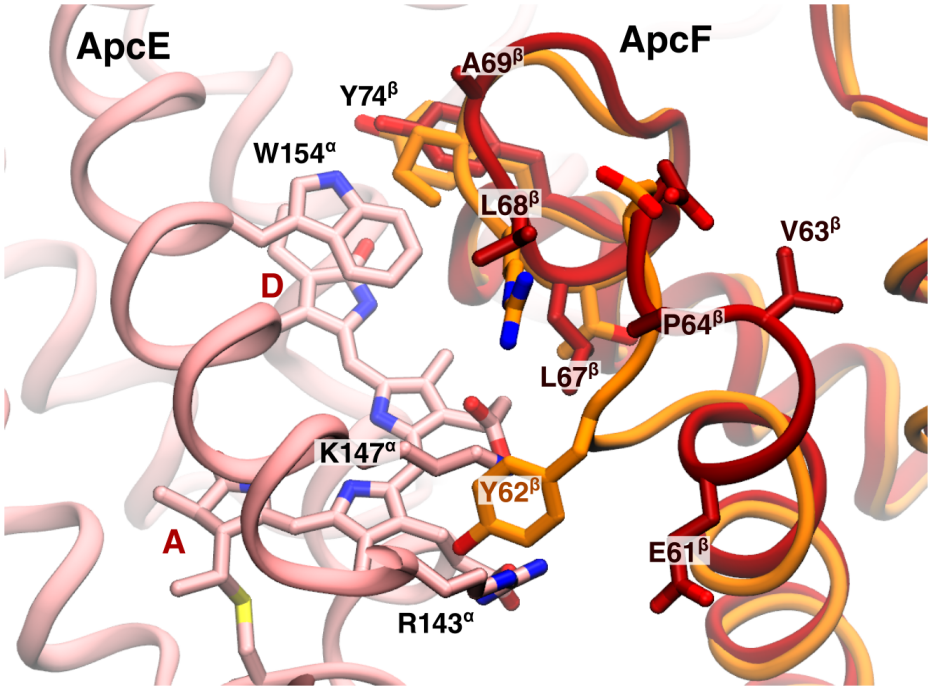

Fig. S9 Interface between ApcE (pink) and ApcF (dark red) at the level of the ApcE pigment. The ApcB chain (orange) is superimposed to ApcF for comparison. The amino acids of ApcF that are substituted or missing in ApcB are indicated, and labeled according to the ApcF sequence (note that ApcF has the additional residue E61 in the sequence). The ApcB residues clashing with ApcE atoms (Y62 and Y74) are also shown, together with the close ApcE residues (R143, K147, and W154)

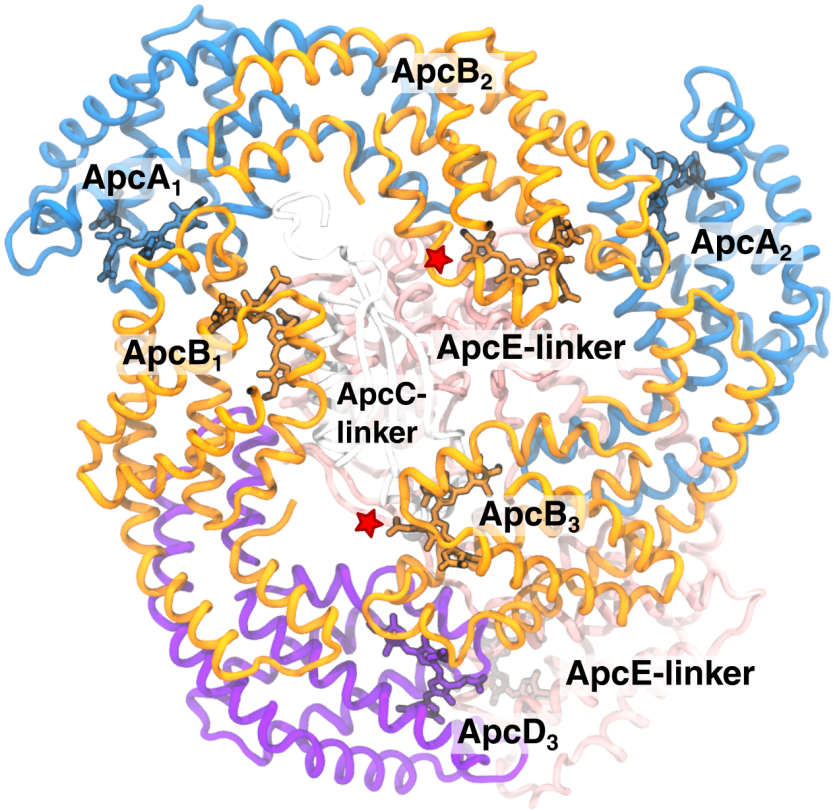

Fig. S10 Interactions between the ApcE-linker and the **D-trimer**. This figure is the same as Figure 1c in the main text, but here the ApcE-linker is also shown (pink). The red stars indicate regions close to the pigments where ApcB and ApcE-linker are in contact.

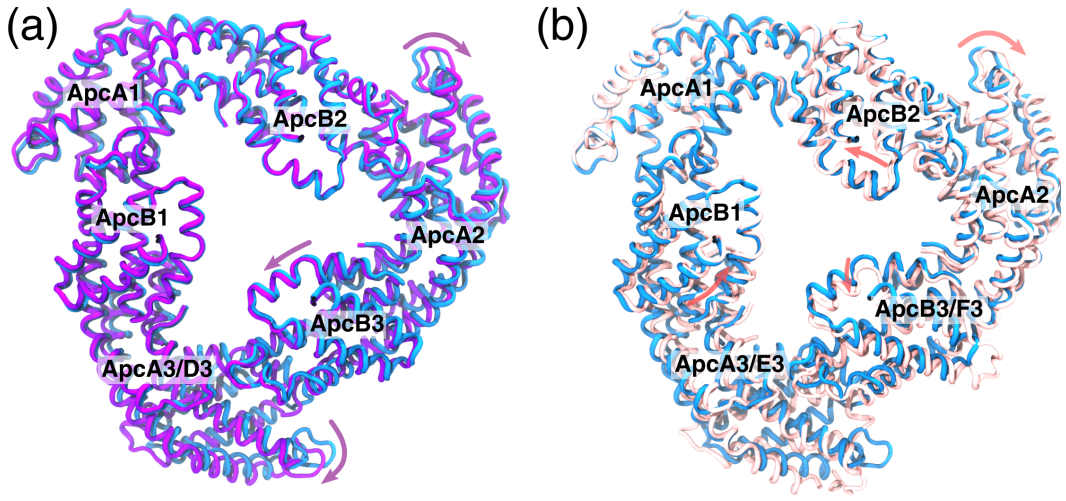

Fig. S11 Structural superposition of the TE trimers with the **AB-trimer**. (a) **D-trimer** (violet) vs **AB-trimer** (blue). (b) **EF-trimer** (pink) vs **AB-trimer** (blue). The orientation and chain labeling are the same as in Figure **??** of the main text. Pigments and linker chains/domains are not shown. The arrows indicate the major global structural differences passing from the **AB-trimer** to each TE trimer (changes in ApcE are not indicated).

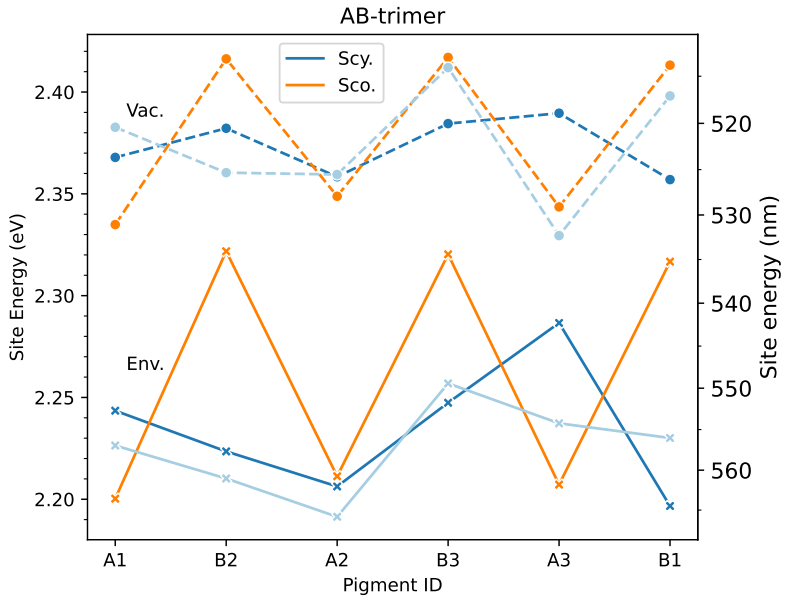

Fig. S12 Comparison of the site energies in the two **AB-trimers** of **Scy. 6803** (blue lines). The site energies of **Sco. 7002** are also given for reference.

S4 Additional tables

Table S2 Exciton Hamiltonians for the Apc trimers in **Sco. 7002** (left) and **Scy. 6803** (right)

Sco. 7002 AB-trimer

	$\mathbf{ApcA_1}$	$\mathbf{ApcB_1}$	$\mathbf{ApcA_2}$	$\mathbf{ApcB_2}$	$\mathbf{ApcA_3}$	$\mathbf{ApcB_3}$
$\mathbf{ApcA_1}$	17747	−90.9	1.9	10.8	2.1	3.9
$\mathbf{ApcB_1}$	—	18685	3.8	7.9	11.5	6.7
$\mathbf{ApcA_2}$	—	—	17835	−90.5	1.9	11.2
$\mathbf{ApcB_2}$	—	—	—	18727	4.4	9.1
$\mathbf{ApcA_3}$	—	—	—	—	17802	−87.4
$\mathbf{ApcB_3}$	—	—	—	—	—	18714

Scy. 6803 AB-trimer

	$\mathbf{ApcA_1}$	$\mathbf{ApcB_1}$	$\mathbf{ApcA_2}$	$\mathbf{ApcB_2}$	$\mathbf{ApcA_3}$	$\mathbf{ApcB_3}$
$\mathbf{ApcA_1}$	18095	−89.9	2.2	10.8	2.0	3.9
$\mathbf{ApcB_1}$	—	17718	3.6	6.6	10.5	9.1
$\mathbf{ApcA_2}$	—	—	17795	−95.5	2.3	11.1
$\mathbf{ApcB_2}$	—	—	—	17934	2.9	7.5
$\mathbf{ApcA_3}$	—	—	—	—	18443	−98.9
$\mathbf{ApcB_3}$	—	—	—	—	—	18127

Sco. 7002 D-trimer

	$\mathbf{ApcA_1}$	$\mathbf{ApcB_1}$	$\mathbf{ApcA_2}$	$\mathbf{ApcB_2}$	$\mathbf{ApcD_3}$	$\mathbf{ApcB_3}$
$\mathbf{ApcA_1}$	17755	−97.0	2.3	11.2	2.4	4.5
$\mathbf{ApcB_1}$	—	17593	3.9	8.4	12.7	10.2
$\mathbf{ApcA_2}$	—	—	18031	−93.6	2.4	10.7
$\mathbf{ApcB_2}$	—	—	—	17894	4.3	12.9
$\mathbf{ApcD_3}$	—	—	—	—	17605	−97.6
$\mathbf{ApcB_3}$	—	—	—	—	—	17704

Scy. 6803 D-trimer

	$\mathbf{ApcA_1}$	$\mathbf{ApcB_1}$	$\mathbf{ApcA_2}$	$\mathbf{ApcB_2}$	$\mathbf{ApcD_3}$	$\mathbf{ApcB_3}$
$\mathbf{ApcA_1}$	18189	−96.4	2.4	11.0	2.5	4.2
$\mathbf{ApcB_1}$	—	17524	3.8	9.6	12.3	12.1
$\mathbf{ApcA_2}$	—	—	18176	−93.3	2.5	10.4
$\mathbf{ApcB_2}$	—	—	—	17551	4.1	13.4
$\mathbf{ApcD_3}$	—	—	—	—	17618	−96.9
$\mathbf{ApcB_3}$	—	—	—	—	—	17872

Sco. 7002 EF-trimer

	$\mathbf{ApcA_1}$	$\mathbf{ApcB_1}$	$\mathbf{ApcA_2}$	$\mathbf{ApcB_2}$	$\mathbf{ApcE_3}$	$\mathbf{ApcF_3}$
$\mathbf{ApcA_1}$	17640	−92.8	2.2	12.1	1.8	4.0
$\mathbf{ApcB_1}$	—	17905	4.6	13.8	9.7	10.2
$\mathbf{ApcA_2}$	—	—	17677	−90.7	2.0	11.6
$\mathbf{ApcB_2}$	—	—	—	17706	4.1	8.7
$\mathbf{ApcE_3}$	—	—	—	—	17326	−68.1
$\mathbf{ApcF_3}$	—	—	—	—	—	17701

Scy. 6803 EF-trimer

	$\mathbf{ApcA_1}$	$\mathbf{ApcB_1}$	$\mathbf{ApcA_2}$	$\mathbf{ApcB_2}$	$\mathbf{ApcE_3}$	$\mathbf{ApcF_3}$
$\mathbf{ApcA_1}$	17849	−97.0	2.2	12.2	1.9	3.9
$\mathbf{ApcB_1}$	—	17853	4.3	11.2	10.5	9.9
$\mathbf{ApcA_2}$	—	—	17651	−97.7	2.2	11.1
$\mathbf{ApcB_2}$	—	—	—	17673	4.1	9.0
$\mathbf{ApcE_3}$	—	—	—	—	17581	−76.3
$\mathbf{ApcF_3}$	—	—	—	—	—	17882

References

1 P. P. Peng, L. L. Dong, Y. F. Sun, X. L. Zeng, W. L. Ding, H. Scheer, X. Yang and K. H. Zhao, *Acta Crystallogr. Sect. D Biol. Crystallogr.*, 2014, **70**, 2558–2569.